International Journal of Pavement Engineering

ISSN: 1029-8436 (Print) 1477-268X (Online) Journal homepage: http://www.tandfonline.com/loi/gpav20

Performance modelling of a solar road panel prototype using finite element analysis

Andrew B. Northmore & Susan L. Tighe

To cite this article: Andrew B. Northmore & Susan L. Tighe (2016) Performance modelling of a solar road panel prototype using finite element analysis, International Journal of Pavement Engineering, 17:5, 449-457, DOI: 10.1080/10298436.2014.993203

To link to this article: http://dx.doi.org/10.1080/10298436.2014.993203

Published online: 23 Dec 2014.

International Journal of Pavement Engineering, 2016
Vol. 17, No. 5, 449–457, http://dx.doi.org/10.1080/10298436.2014.993203

Performance modelling of a solar road panel prototype using finite element analysis

Andrew B. Northmore* and Susan L. Tighe

Civil and Environmental Engineering, University of Waterloo, 200 University Ave West, Waterloo, ON, Canada N2L 3G1

(*Received 2 November 2014; accepted 23 November 2014*)

Performance prediction is a critical step towards the acceptance of a new pavement structure. This is true for both conventional and innovative designs; however, it is particularly important for innovative designs that attempt to redefine pavement design practices. One such innovative design concept is the solar road panel; a road panel with a transparent surface that generates electricity through embedded solar cells. Despite the work completed by multiple organisations towards the development of this concept, questions exist about the viability of these panels as a structural pavement surface. This paper investigates these questions through a finite element modelling approach that assesses a prototype panel's performance on a variety of structural bases. Overall, this paper finds that it is possible to design a solar road panel to withstand traffic loading and that a concrete structural base allows for substantial optimisation to the analysed prototype design.

Keywords: solar road panel; finite element modelling; innovative design; performance modelling; sustainable pavements

1. Introduction

Pavements have been constructed out of the same materials for the last century for a very simple reason; asphalt and concrete are both proven performers under the structural loads and environmental conditions that pavements are subjected to (TAC 2013). As a result, recent endeavours to make pavements more sustainable have focused on slightly tweaking this working formula; substantial changes that move away from a concrete or asphalt driving surface carry inherent risks that must first be mitigated through thorough analysis.

This analysis usually starts with laboratory and numerical analysis components. Lab testing is important to identify the characteristics of the new structure being assessed, but this often cannot replicate the conditions that actual pavements see in the field. Extrapolating the lab results using finite element (FE) or empirical methods allows engineers to up-scale their testing to the realm of *in situ* conditions and make predictions about the performance of their structures in the field before undertaking costly *in situ* testing.

This analysis process is being used in the development of solar road panel systems; modular solar photovoltaic panels specially designed to withstand the structural and environmental loads subjected on pavements. Such innovative design projects require detailed analysis to prove field performance before *in situ* testing. This analysis began with a thorough structural evaluation and FE modelling to predict *in situ* performance.

1.1. *Objectives and scope*

The objective of this paper is to determine the structural performance of a solar road panel prototype installed on concrete, asphalt, granular and subgrade structural bases when subjected to static tyre loads using FE analysis. This modelling will demonstrate the structural base conditions required for successful installation of a solar road panel network.

The basis of this analysis is the FE model of a prototype solar road panel developed by the Centre for Pavement and Transportation Technology (CPATT) at the University of Waterloo (Northmore 2014). The structural bases will be designed based on the typical pavement structures in Ontario, Canada; however, this framework is easily adaptable to other locations by modifying the material properties used in the modelling to local values.

2. Literature review

The literature review covers a summary of the solar road panel design concept, the structure of the panel being studied, the FE model of the panel being studied and the typical assumptions used in the FE modelling of pavement structures.

2.1. *Solar road panel design concept*

Solar road panel prototypes have been developed by three organisations, including CPATT, Solar Roadways (Solar Roadways 2013) and TNO (TNO 2013). These devices were all designed around a similar concept as shown in

*Corresponding author. Email: anorthmo@uwaterloo.ca

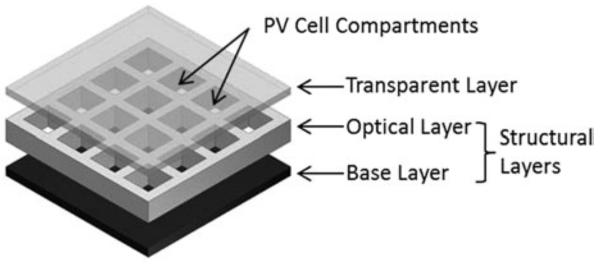

Figure 1. Exploded view of the solar road panel conceptual design (Northmore and Tighe 2012).

Figure 1 where there were three material layers that bypass load around embedded solar cells and onto a structural base beneath the panel.

The panel constructed at CPATT, the basis for the analysis in this paper, used two laminated 10-mm panes of tempered glass for the transparent layer, while the optical and base layers were made of 12.7-mm and 19.1-mm thick GPO-3 fibreglass respectively. The optical layer was made of ribbing to allow space for 125-mm solar cells to be installed while the base was a solid block of cast fibreglass. An image of this panel, with an aluminium c-channel housing, is shown in Figure 2.

2.2. *Solar road panel FE model*

Extensive flexural testing and FE modelling demonstrated that the solar road panel prototype developed by CPATT was best modelled as a series of shell elements with the following material properties: Tempered Glass, 75-GPa Elastic Modulus, 0.30 Poisson's Ratio; GPO-3, 13-GPa Elastic Modulus, 0.32 Poisson's Ratio (Northmore 2014). These values were on the upper bound of material properties obtained from literature on both tempered glass (Alsop and Saunders 1999, ACI 2013) and GPO-3 fibreglass (ACI 2013, Rochling 2013).

2.3. *Pavement FE modelling*

Typical pavement design follows an empirical or mechanistic-empirical process; however, some specialty applications involve FE analysis. These cases provide validated, simplified models that approximate the performance of a given pavement structure.

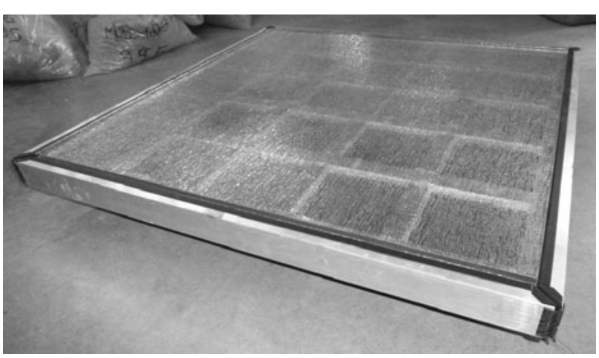

Figure 2. CPATT solar road panel prototype.

To do this, two assumptions are often made. The first is that the materials are elastic, a valid simplification for determining static response but does not account for cyclic loading induced deformations to a pavement structure. The second is that the material properties in each layer are homogenous, which assumes a high degree of competency in construction. These factors are demonstrated in work by Caliendo and Parisi (2010), Cho *et al.* (1996), Greene *et al.* (2010), Mak (2012) and Xia (2010).

3. Methodology

To assess the performance of the solar road panel prototype, half-axle loads were applied to the panel on varying structural bases using Abaqus CAE 6.11. The details for this are outlined as follows.

3.1. *Load conditions and cases*

Two load cases were considered for the FE analysis as shown in Table 1. The static load was based on the maximum single wheel load under Canadian regulations (CSA 2006), while the fatigue load was an equivalent single axle load. The contact area for the fatigue load was determined using the geometric relations to convert dual tyre loads to singles for concrete pavement section analysis (Huang 2004) and an assumed tyre pressure of 600 kPa. It was assumed that these correlations were relevant to solar road panels due to the similarity of their material properties to concrete. Both loads were applied as pressures on the panel surface with an even distribution of the total force.

The loads were applied to four different areas on the panel in order to determine how this affected performance. The locations were, as shown in Figure 3, the centre, transverse edge, longitudinal edge and corner of the panel.

3.2. *Structural base FE models*

The structural design and material property assumptions for the bases are outlined in Table 2; where 'PCC' refers to concrete, 'HMA' refers to asphalt, 'G' refers to granular and 'SG' refers to subgrade. The structural designs were based on the 1000 AADTT typical pavement designs for Ontario from ARA's StreetPave report (2011). The

Table 1. Static and fatigue load cases.

Condition	Load (kN)	Contact dimensions
Static	87.5	0.60 m × 0.25 m
Fatigue	40	0.529 m × 0.364 m

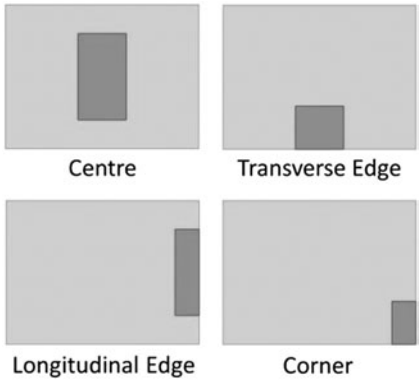

Figure 3. FE tyre load application locations, direction of travel up the page.

granular and subgrade bases were based on the HMA pavement structure base with layers removed accordingly.

The material properties identified in Table 2 were derived from Ontario's default parameters for the AASHTOWare pavement design tool (MTO 2012), Ontario provincial standards for granular materials (OPSS 2003), StreetPave report (ARA 2011), Canadian Pavement Asset Design and Management Guide (TAC 2013) and the AASHTO Guide for Design of Pavement Structures (AASHTO 1993). These documents represented the standard design practice for Ontario pavement structures, so no variability of these values was considered in the study.

3.3. *Modelling techniques and validation*

Each layer was modelled as a three-dimensional solid extrusion with homogenous material properties. Contact between layers were defined as normal contact with a linear over-closure penalty and automatic stabilisation control, as recommended by the Abaqus user manual (2013).

The dimensions and mesh sizing of the base layers were validated to ensure 95% accuracy of modelling on a one-fourth base model with symmetry applied on the two inside faces of the pavement depth and encastre conditions on the outside faces. Symmetry was also assumed in the panel model to simplify modelling requirements as applicable. Mesh seeding within the base layers was single biased towards the loaded corner and double biased towards the contact surfaces for each layer as shown in Figure 4.

As required, the step size was decreased to improve the probability of a converging solution. This was done upon the recommendation of the existing literature (Mak 2012).

3.4. *Fatigue life analysis methods*

The fatigue life models in the analysis were dependent on the material being assessed. These models are described herein.

Glass specimens fail through fracture methods which were well documented for varying glass chemistries in the literature (Alsop and Saunders 1999). Particularly with tempered glass, as used in this prototype, any cracks that develop past the tempered layer would propagate rapidly and cause the glass to fail. It was therefore important for the fatigue life of the panel to keep tensile strain in the transparent layer below the 69-MPa compressive stress developed on the faces of the glass panes through the tempering process.

Fibreglass fails through traditional fatigue theory methods, with S-N curves available to model this behaviour (Demers 1998). These theories do present endurance limits that, for most fibre reinforced materials, allow infinite stress cycles so long as stresses are below 0.3 times the ultimate strength of the material. For the GPO-3 being used in this study, this endurance limit was 16.6 MPa.

Concrete pavements fail by a number of mechanisms depending on the ratio of the applied stress to the compressive strength of the material. These equations are demonstrated in Huang (2004) and also include an endurance limit of 0.45 times the compressive strength. Assuming a conventional compressive strength of 32 MPa in the base layer concrete, this would allow localised stresses of up to 14.4 MPa.

Asphalt materials fail from structural loading through two main mechanisms: fatigue cracking and rutting. Both of these mechanisms have been empirically related to a number of allowable load cycles through the elastic modulus of the asphalt and the horizontal strain at the bottom of the asphalt layer, for fatigue cracking, or the vertical strain at the bottom of the lowest granular layer,

Table 2. Structural base designs and material properties.

	Base structure (mm)				Material properties		
Material	PCC	HMA	G	SG	Elastic/resilient modulus (MPa)	Poisson's ratio	Specific density (kg/m^3)
PCC	200	–	–	–	29,600	0.20	2320
HMA	–	120	–	–	2758	0.35	2460
G-A	200	150	150	–	250	0.35	2400
G-B	–	300	300	–	200	0.35	2000
SG	Infinite				50	0.30	1750

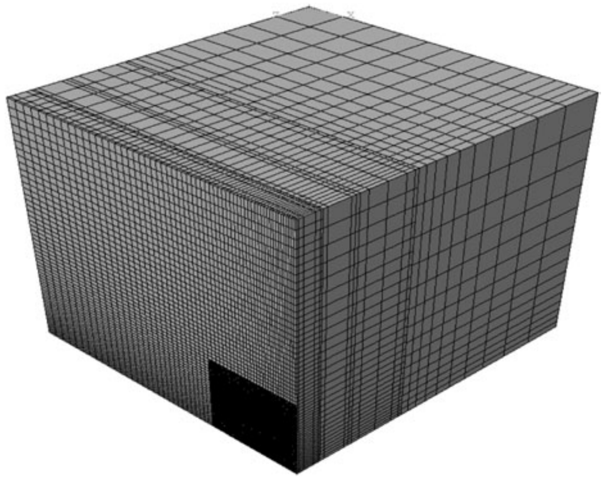

Figure 4. Meshing strategy for a centre load test with an HMA base.

for rutting (Huang 2004). As a result, lower strains are desirable at both of these locations in order to promote longer design lives of HMA pavements.

4. Static and fatigue load simulation results

The FE modelling resulted in stress profiles as shown in Figure 5, representing the stress contour on the transparent layer under static load on the centre of a panel with an HMA base. The highest stresses were located under the centre of the tyre, which was centred at the bottom right corner of the specimen in the image, with a second stress peak above it. This was due to the ribbing of the optical layer beneath the transparent layer, allowing the glass to deflect freely in areas over the solar cells but not over the fibreglass ribbing.

Similar profiles were observed with the fatigue load cases, as shown in Figure 6 for the same scenario as Figure 5; however, the stresses were distributed farther into the width of the section. This was due to the larger footprint of the fatigue load, as it was simulating a dual tyre so it covered a larger area. As a result, local stresses also reached maxima in the adjacent two solar cell pockets in the optical layer.

Stresses in the base layer were distributed as shown in Figure 7, where the stress concentrations were located under the optical layer ribbing. This was expected as the ribbing was the transmission medium for the load from the transparent layer to the base layer.

The profile for all of the stress contours were very similar, though the scale of the stresses varied depending on the load configuration and structural base. Figure 8 shows the maximum stress measured in the transparent layer when it was subjected to the fatigue load. This figure demonstrates two key results: the performance ranking of panels on different bases and the performance of tyre loading on varying locations.

Figure 8 demonstrated that the ranking of the structural bases from lowest to highest maximum stresses generated in the panel was as follows: concrete, asphalt, granular, subgrade. This was the expected result from a pavement

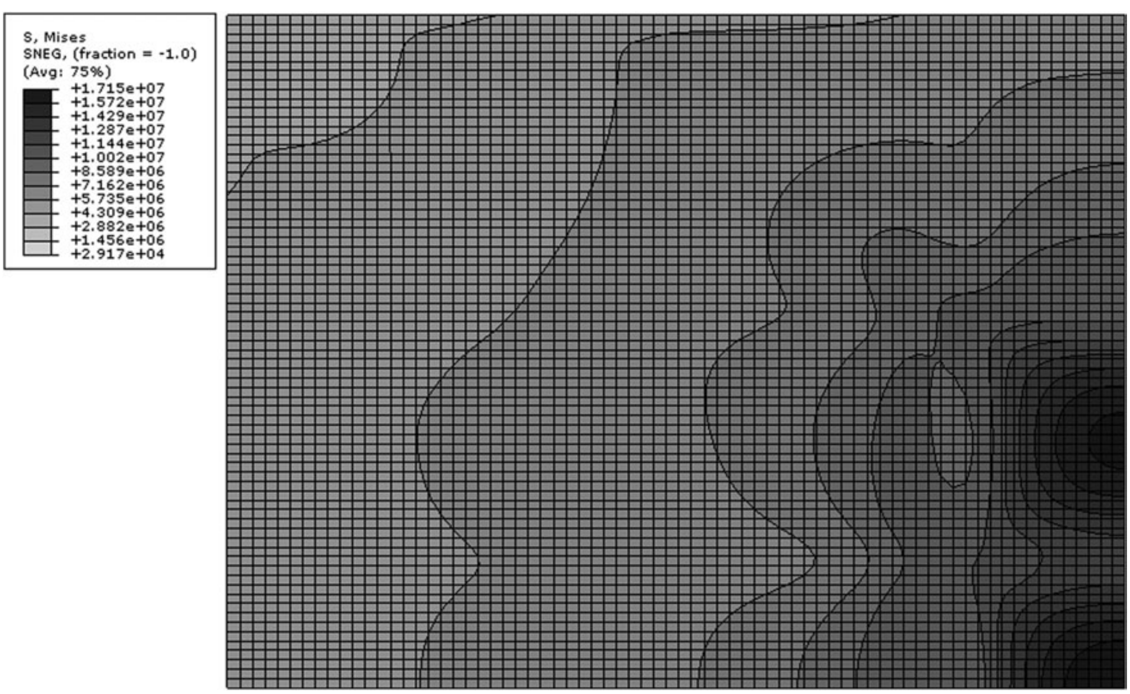

Figure 5. Transparent layer stress contours under static, centre load with HMA base.

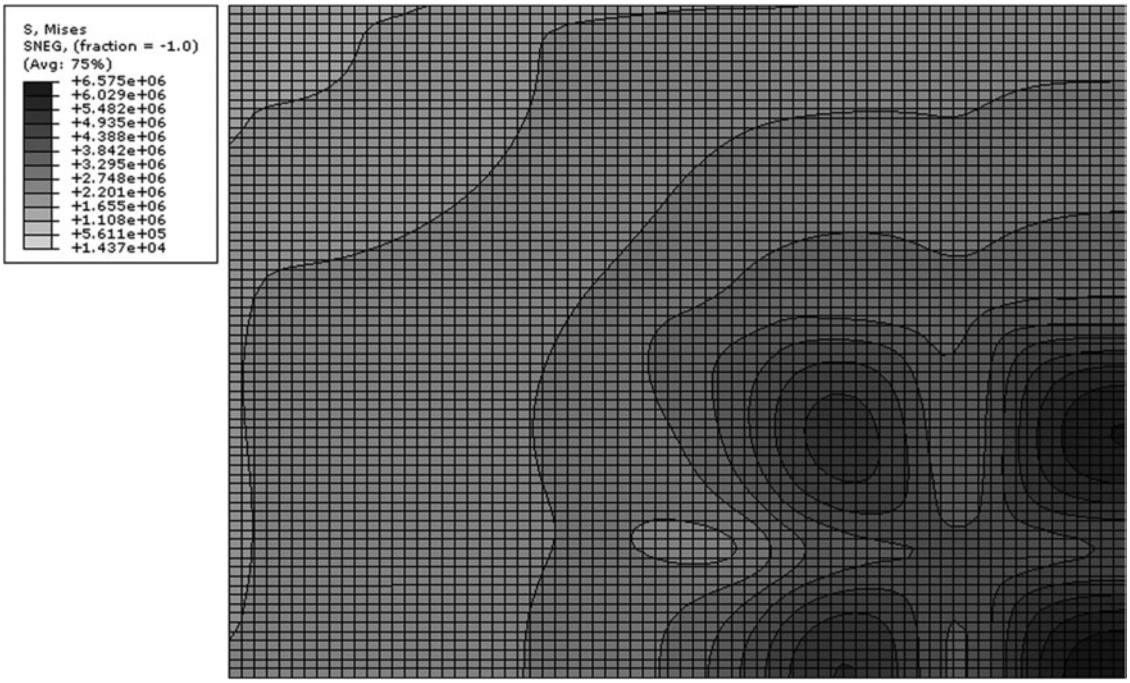

Figure 6. Transparent layer stress contours under fatigue, centre load with HMA base.

engineering perspective as this is also the ranking of these structures from the least flexible to the most flexible. Concrete pavements are known for their rigidity and effective load distribution, while asphalt pavements are more flexible and allow for more local loading through the structure. This local loading translated to greater pavement deflections, which in this case allowed the panel to deflect further and develop greater stresses. This same phenomenon occured for the granular and subgrade layers but to greater extents.

Figure 8 also demonstrated that the centre loading allowed the highest stresses to develop in each scenario

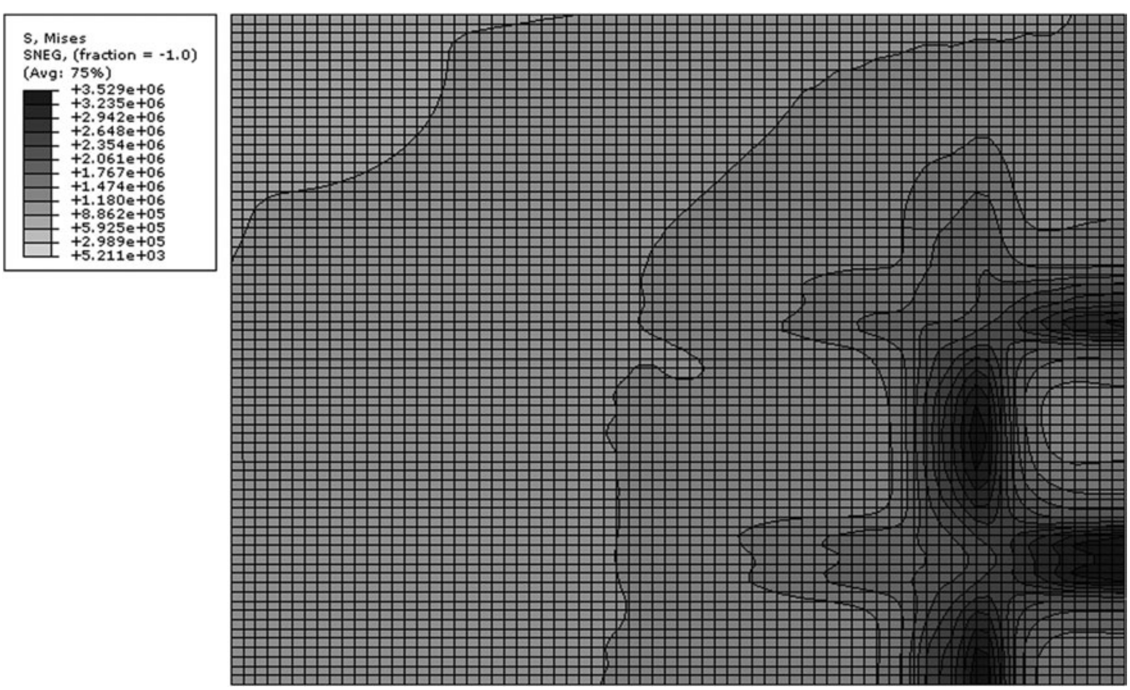

Figure 7. Base layer stress contours under static, centre load with HMA base.

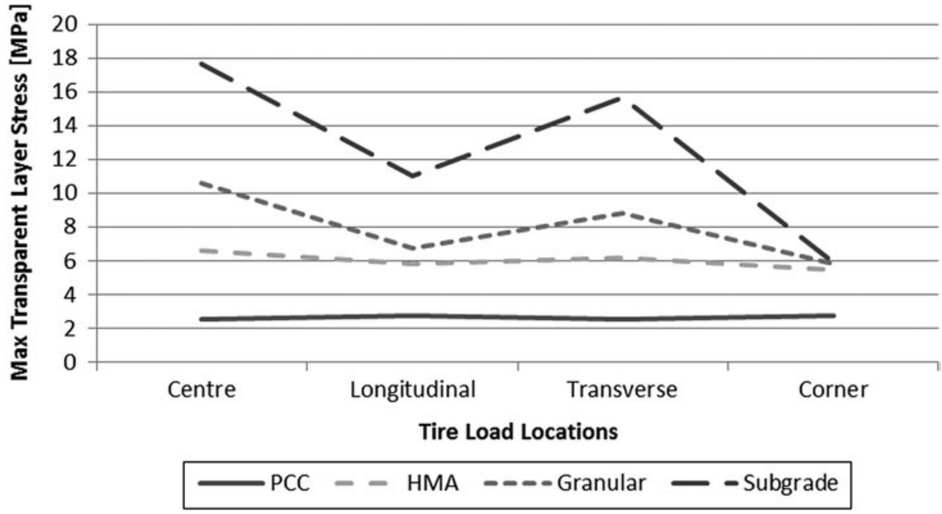

Figure 8. Transparent layer stress when subjected to fatigue load.

while the corner loading had the lowest stresses. This was due to the location of the ribbing within the optical layer. In the centre load case there were no ribs located directly beneath the centre of the tyre, so the peak load from the tyre was able to deflect unsupported glass and, therefore, create higher stresses. In the corner load there were two ribs crossing under the centre of the tyre load, providing more reinforcement against these deflections. This is further validated in Figure 9, which shows that the stress maxima were offset from the corner of the panel in the transparent layer with a corner load application.

5. Fatigue life analysis

The fatigue life analysis was divided into sections for the prototype panel, concrete structural base and the asphalt structural base.

5.1. *Prototype panel*

Figure 10 shows the maximum stress obtained in the transparent layer from all iterations of the simulations. As demonstrated, the stress was never greater than 69 MPa, which was the endurance limit for tempered glass.

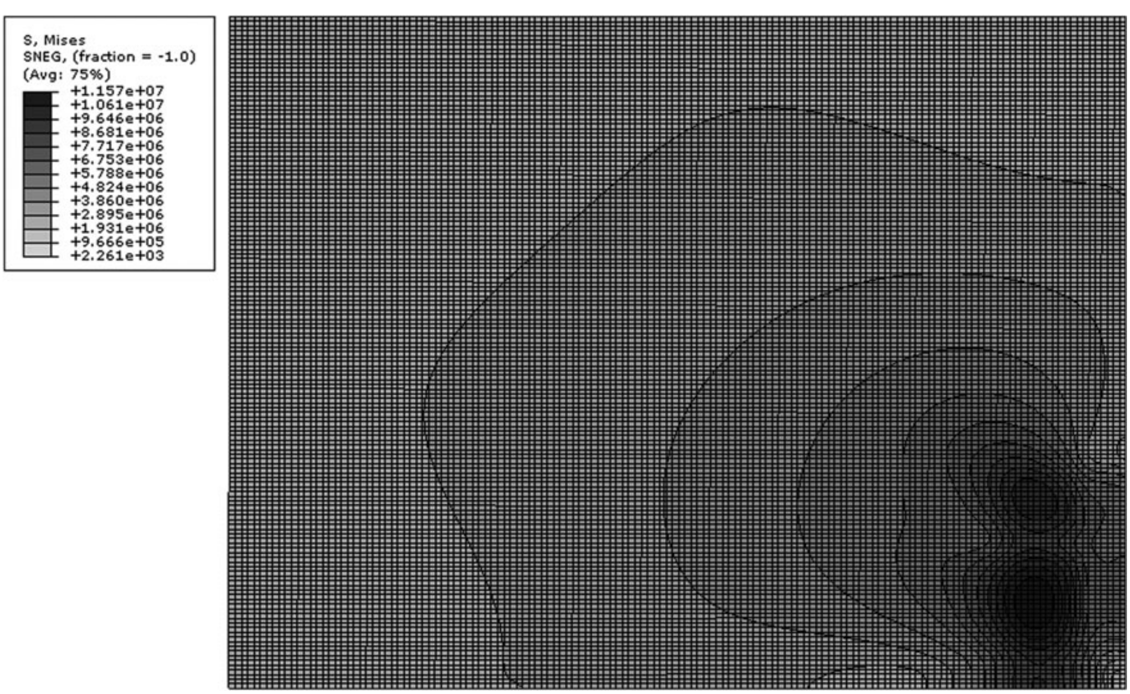

Figure 9. Transparent layer stress contours under static, corner load with HMA base.

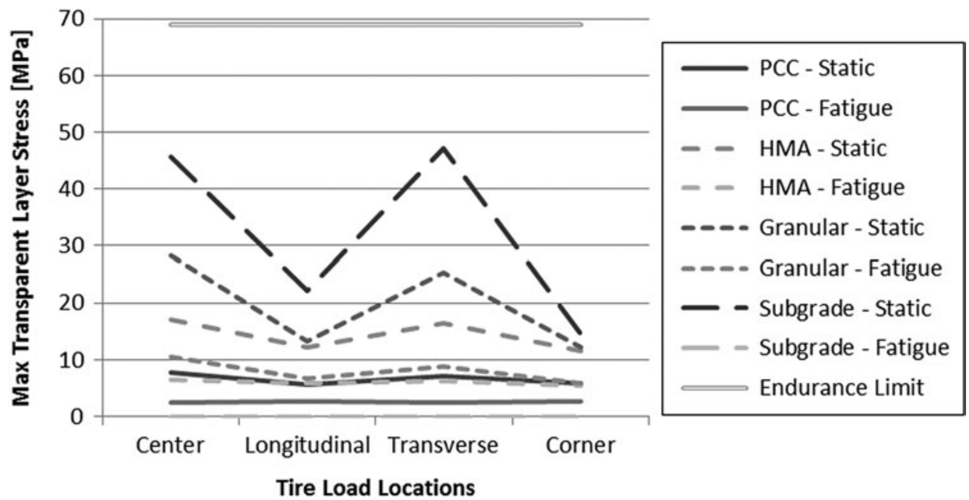

Figure 10. Transparent layer fatigue life endurance limit check.

This indicated that the transparent layer should have infinite life in this current design, barring local defects.

Figure 11 then shows the maximum stress that was obtained in the base layer of the prototype from all iterations of the simulations. Much like the glass layer, the endurance limit of the fibreglass was never reached in any condition, so overall it was found that the current panel design would likely not fail due to fatigue.

5.2. *Concrete structural base layer*

The concrete structural base endurance limit check is shown in Figure 12, where it was demonstrated that under no conditions did the stress applied to the concrete base reach the maximum 14.4-MPa level. As concrete pavements are typically designed with this stress threshold in mind, this was the expected result.

5.3. *Asphalt structural base layer*

Figure 13 shows the maximum horizontal strain obtained at the bottom of the asphalt layer from the fatigue load, which is the variable parameter for determining fatigue cracking life. As there was no endurance limit, the same model was run without the panel to determine a control sample with just the asphalt base structure to compare the strains to. Figure 13 shows that, in all cases, the strain measured with the panel installed was either similar to or less than that of the control sample, so installing a solar

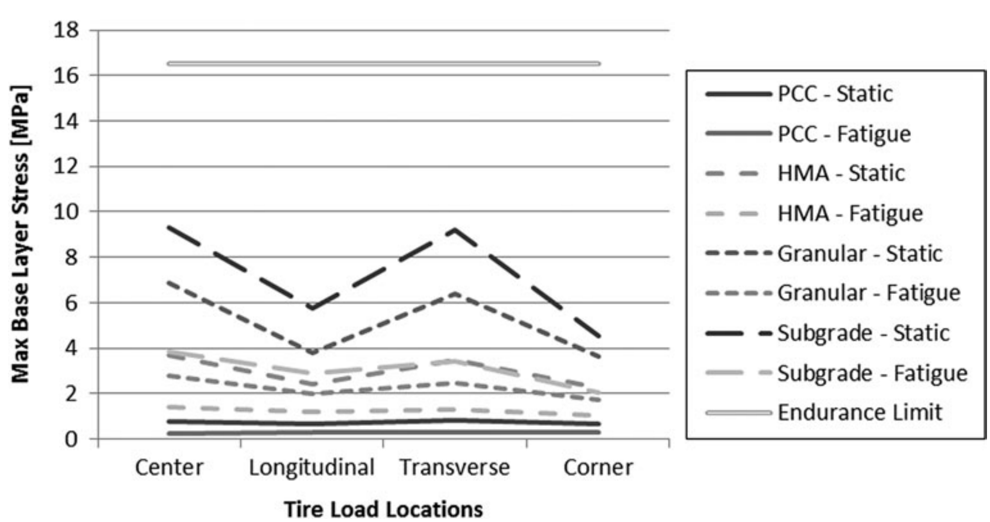

Figure 11. Base layer fatigue life endurance limit check.

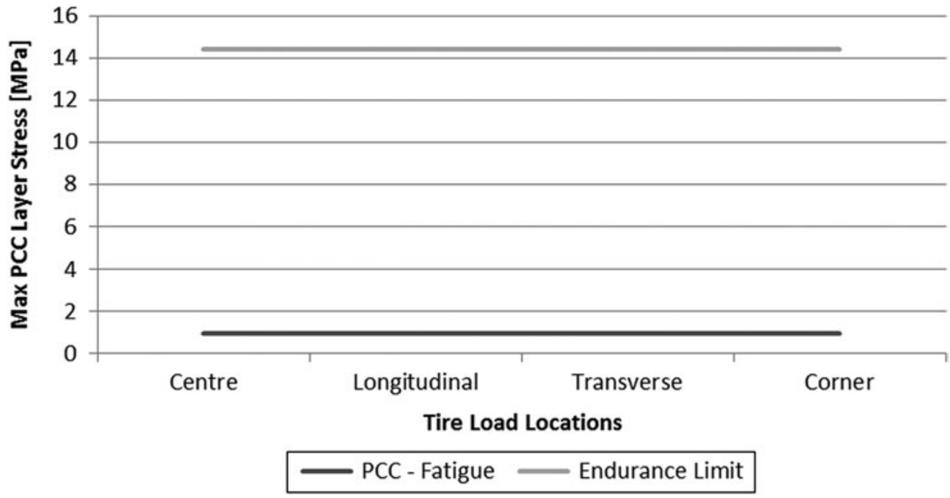

Figure 12. Concrete layer fatigue life endurance limit check.

road panel would either improve or maintain the fatigue cracking life of the asphalt base.

Similarly, Figure 14 shows the maximum vertical compressive strain obtained at the bottom of the Granular B layer in the asphalt structural base, which was indicative of rutting. Again the modelled strains were far less than the control strain, indicating an improved rutting life of the asphalt structural base.

6. Conclusions

This research resulted in two major conclusions: it is possible to build a solar road panel that can withstand traffic loading and solar road panels either maintain or improve the expected structural performance of the base they are installed on.

By demonstrating that the stresses obtained in the transparent and base layers were well under the endurance limits for their materials, it was found that the solar road panel that was designed and tested for this analysis is a structurally sound panel for pavement applications. This allows for two major events in the design process: *in situ* testing and design optimisation. The characterisation of the panel demonstrates that *in situ* testing is a feasible next step, from a structural perspective, for determining the performance model for a solar road panel. Also, design refinements can be made to reduce the cost of the panel while still keeping the developed panel stresses below their endurance limits.

It was also demonstrated that the additional reinforcement supplied by a solar road panel further distributed tyre loads around the base materials and improved their design lives. This allows for optimisation of the structural base design in-line with the panel design optimisation to further reduce cost and improve panel sustainability. Concrete was also identified as the base with the most opportunities

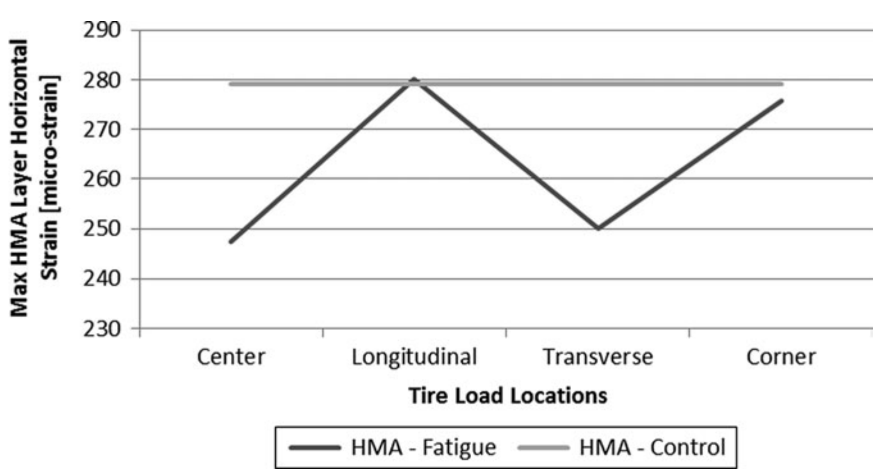

Figure 13. Asphalt base layer maximum horizontal strain.

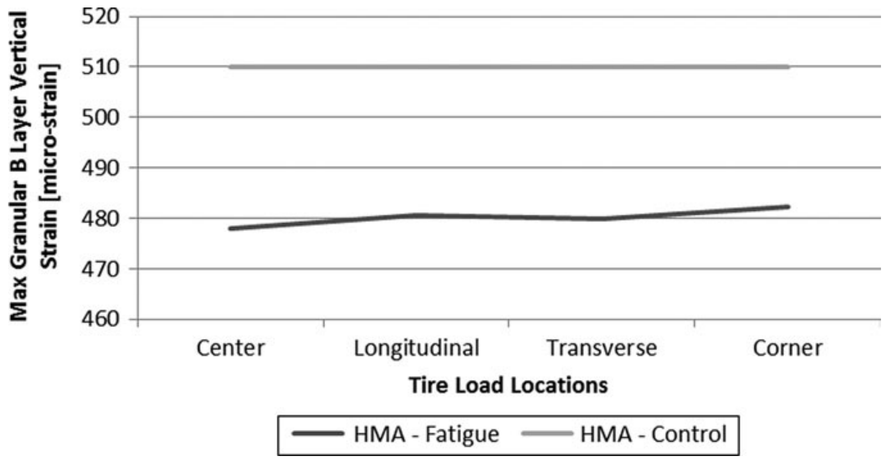

Figure 14. Asphalt base maximum vertical compressive strain in the Granular B layer.

for base design and panel design improvements, so this is the base of choice for solar road panel installations.

Acknowledgements

The authors would like to thank the Natural Science and Engineering Research Council of Canada, Ontario Graduate Scholarship Program, University of Waterloo, Transportation Association of Canada and the Norman W. McLeod Chair in Sustainable Pavement Engineering for their continued support towards this research programme.

References

AASHTO, 1993. *AASHTO guide for design of pavement structures*. Washington, DC: AASHTO.

Abaqus, 2013. *Abaqus CAE 6.13 documentation*. Providence, RI: Dassault Systems.

ACI, 2013. *Matweb material property data*. Available from: http://www.matweb.com/index.aspx

Alsop, D.J.A. and Saunders, R.J., 1999. *Structural use of glass in buildings*. London: Institute of Structural Engineers.

ARA, 2011. *Methodology for the development of equivalent structural design matrix for municipal roadways*. Toronto, ON: Ready Mix Concrete Association of Ontario.

Caliendo, C. and Parisi, A., 2010. Stress-prediction model for airport pavements with jointed concrete slabs. *Journal of Transportation Engineering*, 136 (7), 664–677.

Cho, Y.H., McCullogh, B.F., and Weissmann, J., 1996. Considerations on finite-element method application in pavement structural analysis. *Transportation Research Record: Journal of the Transportation Research Board*, 1539, 96–101.

CSA, 2006. *Canadian highway bridge design code*, CAN/CSA-S6 CL-625-ONT. Toronto, ON: CSA International.

Demers, C.E., 1998. Fatigue strength degradation of E-glass FRP composites and carbon FRP composites. *Construction and Building Materials*, 12 (1998), 311–318.

Greene, J., *et al.*, 2010. Impact of wide-base single tires on pavement damage. *Transportation Research Record: Journal of the Transportation Research Board*, 2155, 82–90.

Huang, Y.H., 2004. *Pavement analysis and design*. 2nd ed. Upper Saddle River, NJ: Pearson Prentice Hall.

Mak, T.L.A., 2012. *Modular road plate system*, Thesis (MASc). University of Waterloo.

MTO, 2012. *Ontario's default parameters for AASHTOWare pavement ME design interim report*. Toronto: Ministry of Transportation Ontario.

Northmore, A.B., 2014. *Canadian solar road panel design: a structural and environmental analysis*, Thesis (MASc). University of Waterloo.

Northmore, A.B. and Tighe, S.L., 2012. Developing innovative roads using solar technologies. *9th international transportation specialty conference*, 6–9 June 2012. Edmonton, Alberta, Canada: Canadian Society of Civil Engineering.

OPSS, 2003. *Material specification for aggregates – base, subbase, select subgrade, and backfill material*, No. OPSS 1010. Ontario Provincial Standard Specification.

Rochling, 2013. *Grade UTR arc/track & flame resistant laminate*. Cleveland, OH: Rochling Glastic Composites.

Solar Roadways, 2013. Solar roadways – a real solution. Available from: http://www.solarroadways.com/main.html

TAC, 2013. *Pavement asset design and management guide*. Ottawa: Transportation Association of Canada.

TNO, 2013. SolaRoad combines road and solar cells. Available from: http://www.tno.nl/content.cfm?context=thema&content=inno_case&laag1=895&laag2=912&item_id=1234

Xia, K., 2010. A finite element model for tire/pavement interaction: application to predicting pavement damage. *International Journal of Pavement Research and Technology*, 3 (3), 135–141.